SANDIA REPORT

SAND2014-15971
Unlimited Release
Printed July 2014

Assessing the standard Molybdenum projector augmented wave VASP potentials.

Ann E. Mattsson

Prepared by
Sandia National Laboratories
Albuquerque, New Mexico 87185 and Livermore, California 94550

Sandia National Laboratories is a multi-program laboratory managed and operated by Sandia Corporation, a wholly owned subsidiary of Lockheed Martin Corporation, for the U.S. Department of Energy's National Nuclear Security Administration under contract DE-AC04-94AL85000.

Sandia National Laboratories

Issued by Sandia National Laboratories, operated for the United States Department of Energy by Sandia Corporation.

Available to DOE and DOE contractors from
U.S. Department of Energy
Office of Scientific and Technical Information
P.O. Box 62
Oak Ridge, TN 37831

Telephone: (865) 576-8401
Facsimile: (865) 576-5728
E-Mail: reports@adonis.osti.gov
Online ordering: http://www.osti.gov/bridge

Available to the public from
U.S. Department of Commerce
National Technical Information Service
5285 Port Royal Rd
Springfield, VA 22161

Telephone: (800) 553-6847
Facsimile: (703) 605-6900
E-Mail: orders@ntis.fedworld.gov
Online ordering: http://www.ntis.gov/help/ordermethods.asp?loc=7-4-0#online

SAND2014-15971
Unlimited Release
Printed July 2014

Assessing the standard Molybdenum projector augmented wave VASP potentials.

Ann E. Mattsson
Multi-Scale Science MS 1322
Sandia National Laboratories
P.O. Box 5800
Albuquerque, NM 87185-1322
aematts@sandia.gov

Abstract

Density Functional Theory (DFT) based Equation of State (EOS) construction is a prominent part of Sandia's capabilities to support engineering sciences. This capability is based on augmenting experimental data with information gained from computational investigations, especially in those parts of the phase space where experimental data is hard, dangerous, or expensive to obtain. A key part of the success of the Sandia approach is the fundamental science work supporting the computational capability. Not only does this work enhance the capability to perform highly accurate calculations but it also provides crucial insight into the limitations of the computational tools, providing high confidence in the results even where results cannot be, or have not yet been, validated by experimental data. This report concerns the key ingredient of projector augmented-wave (PAW) potentials for use in pseudo-potential computational codes. Using the tools discussed in SAND2012-7389 we assess the standard Vienna *Ab-initio* Simulation Package (VASP) PAWs for Molybdenum.

Acknowledgment

This work was supported by the NNSA ASC/PEM program at Sandia. Sandia National Laboratories is a multi-program laboratory managed and operated by Sandia Corporation, a wholly owned subsidiary of Lockheed Martin Corporation, for the U.S. Department of Energy's National Nuclear Security Administration under contract DE-AC04-94AL85000.

Contents

Nomenclature **9**

1 Introduction and Motivation **11**

2 Density Functional Theory **15**

3 The Projector Augmented Wave method **17**

The all-electron calculation 18

Atom configuration 18

The exchange-correlation functional 18

The number of valence electrons 19

The PAW generation 19

The local potential 20

Partial wave cutoffs 20

Number of projectors 21

The valence compensation charge 21

The partial core corrections 21

4 The standard Mo PAWs **23**

Four standard PAW potentials 24

Calculations using the Mo PAW potentials 28

Equilibrium density 28

Pressure 29

Density of States 32

5 Summary and Conclusion **37**

References **38**

List of Figures

1.1 The foundation of Science Based Engineering is to build bridges from the fundamental Laws of Nature up to the Engineering codes, bridging several length and time scales. In this figure two different paths are depicted. The upper one is quite complicated and illustrates the general problem of bridging several different scales. The lower path is already in use at Sandia. For Equation of State construction, data provided by Density Functional Theory (DFT) based calculations are used in addition to experimental data. The DFT calculations are used in two ways, either directly or as a provider of forces in a Molecular Dynamics scheme. 12

2.1 The exact functional would give the exact density, ρ, and thus the exact properties via density functionals, $F[\rho]$. The unknown wave function density functional, $\Psi[\rho]$, would in this case give all properties that can be calculated from the Schrödinger equation exactly. However, the mean field view of using the KS orbitals as approximate electron wave functions would be approximate. Only the density and properties calculated via density functionals are guaranteed to be exact. The quality of a functional can thus not be judged by how well it reproduces wave function derived properties. From Reference 13. 16

4.1 The arctan of the logarithmic derivatives of pseudo wave-functions (colored) compared to those of all-electron wave-functions (black and grey, not seen if the colored points are exactly on top). The RWIGS value of 2.750 (2.600) bohr corresponds to a half nearest neighbor distance in bcc Mo at a density of 8.4 (9.9) g/cm^3. 26

4.2 The arctan of the logarithmic derivatives of pseudo wave-functions (colored) compared to those of all-electron wave-functions (black and grey, not seen if the colored points are exactly on top). The RWIGS value of 2.220 bohr corresponds to a half nearest neighbor distance in bcc Mo at a density of 16 g/cm^3. 27

4.3 The Fermi-Dirac distribution function for a temperature of 50000 Kelvin. . . . 28

4.4 Energy versus volume near equilibrium calculated using different PAW potentials. 29

4.5 The pressure of bcc Mo as a function of density. Note the top scale that gives half the nearest neighbor distance. It is clear that *all* potentials are operating inside their largest core radii in compression, cf. Table 4.1. 31

4.6 DOS at the LDA equlibrium lattice constant calculated using different PAW potentials in VASP and compared to the all-electron RSPt results. Note the ghost states present in the Mo, Mo_pv_02, and Mo_pv_05, PAW potential results. 33

4.7 Integrated DOS at the LDA equlibrium lattice constant calculated using different PAW potentials in VASP and compared to the all-electron RSPt results. Note the ghost states present in the Mo, Mo_pv_02, and Mo_pv_05, PAW potential results. 34

4.8 DOS at 16 g/cm^3 calculated using different PAW potentials in VASP and compared to the all-electron RSPt results. Note the ghost states present in the Mo, Mo_pv_02, and Mo_pv_05, PAW potential results. 35

4.9 Integrated DOS at 16 g/cm^3 calculated using different PAW potentials in VASP and compared to the all-electron RSPt results. Note the ghost states present in the Mo, Mo_pv_02, and Mo_pv_05, PAW potential results. 36

Nomenclature

Dirac The Dirac Equation: The relativistic quantum mechanical wave equation describing electrons in relativistic matter, such as heavy materials like actinides.

SE The Schrödinger Equation: The non-relativistic limit of the Dirac Equation, sufficiently accurate to describe electrons in lighter materials.

DFT Density Functional Theory: The formally exact reformulation of the wave-function based Schrödinger and Dirac Equations in terms of density and currents.

KS The Kohn-Sham Equations: A calculational approach derived from the Dirac/SE using DFT. These are the equations implemented in DFT codes.

Functional A short name for an approximation for the Exchange-Correlation functional which is the only part of DFT that needs to be approximated. The functional sets the possible accuracy of DFT calculations.

LMTO Linear Muffin Tin Orbital: A calculational method used in the RSPt code.

LAPW Linear Augmented Plane Wave: Another calculational method. It is considered the implementation method that gives the most accurate DFT results. Other methods are usually verified against this method.

plane-wave code A code using plane waves as a basis set. This is the computationally most effective approach because Fourier Transforms can be used. Calculations can also be systematically improved by increasing the number of basis functions used, usually specified by the so called 'cut-off'. However, describing core electrons accurately requires a very large cut-off, leading to expensive calculations. The plane-wave approach thus is mostly used together with pseudo-potentials (see below).

all-electron code A code treating all electrons explicitly. LMTO and LAPW codes are all-electron.

pseudo-potential code The chemically inert core electrons are treated in a collective way via pseudo potentials, which increases the computational efficiency considerably. A number of different approaches exist; all are verified by comparing to all-electron, usually LAPW, results.

PAW Projected Augmented Wave: The pseudo potential technique currently considered the most accurate.

RSPt Relativistic Spin-Polarised test: The name of an all-electron, full potential, LMTO code developed by Dr. John M. Wills at Los Alamos National Laboratory.

VASP Vienna *Ab-initio* Simulation Package: A plane wave, pseudo potential (PAW), DFT code extensively used at Sandia.

core electron An electron close to the nucleus. In an LMTO or LAPW treatment these electrons are considered inert and their properties only depend on the closest nuclei. In a pseudo-potential code the effect of the core electrons on the valence electrons is included via pseudo potentials.

semi-core electron An electron that is intermediate between a core and a valence electron. It has the same angular momentum quantum number as some of the valence electrons but has a lower principal quantum number (it is in a lower shell). For the heavier nuclei (or for lighter nuclei at high pressure) these electrons need to be treated as valence electrons.

valence electron The outermost electrons are valence electrons and their properties are dependent on many nuclei. These electrons are forming bonds that hold a solid or molecule together.

Chapter 1

Introduction and Motivation

Density functional theory (DFT) is the preferred computational method for exploring materials properties, and Sandia scientists are at the forefront of DFT-based equation of state (EOS) construction, where information from both experiments and computational investigations are used (See Figure 1.1).

DFT[6,9] is a formally exact reformulation of the Schrödinger Equation (SE) for the ground state of an electron system. Since the DFT equations are far easier to solve than the many-body SE, DFT has become the preferred computational method for exploring properties of materials. One example of a Sandia effort in this area is the recent use of DFT results combined with Z experiments to construct a new Quartz standard leading to resolution of an important discrepancy between flyer plate and laser driven shock data for deuterium.[8] Another example is similar work for Xenon,[21] a material of importance for DOE. Here DFT results helped both in showing that the available Equation of State (EOS) tables were inaccurate at high pressures and in the construction of a new, more accurate, EOS.

For elemental bulk materials with simple structures, such as face-centered cubic (fcc) or body-centered cubic (bcc) atomic arrangements, a computational cell with only one atom can be used. For such simple materials, DFT codes that treats all electrons very precisely can be used, at least at low temperatures. However, for more complicated structures and for calculations at higher temperatures, larger computational cells with more atoms are needed for a good description of the material. For these applications pseudo-potential codes, such as the Vienna *ab-initio* simulation program (VASP),[10,11] have become the workhorse computational tool. In such a code the inert core electrons are replaced by a pseudo-potential (pp) and only the valence electrons are treated explicitly, allowing for more efficient use of computer resources. High quality pseudo-potentials are available for VASP and other codes, the quality usually being determined by comparing zero temperature lattice constants and bulk moduli with results from equivalent calculations with an all-electron code. It is important to note that the quality of a pseudo-potential can only be determined by comparison to all-electron calculations, never by comparison to experiment.

The key issue with pseudo-potentials are their transferability. A pp is usually constructed from the all-electron results of a single, free, spherically symmetric atom. For this atom the pp is generally producing the same results as an all-electron calculation. However, the success of transferring a pp to a different environment, such as to an atom in a bulk lattice, is dependent on a number of factors. Until recently most pps have been constructed for

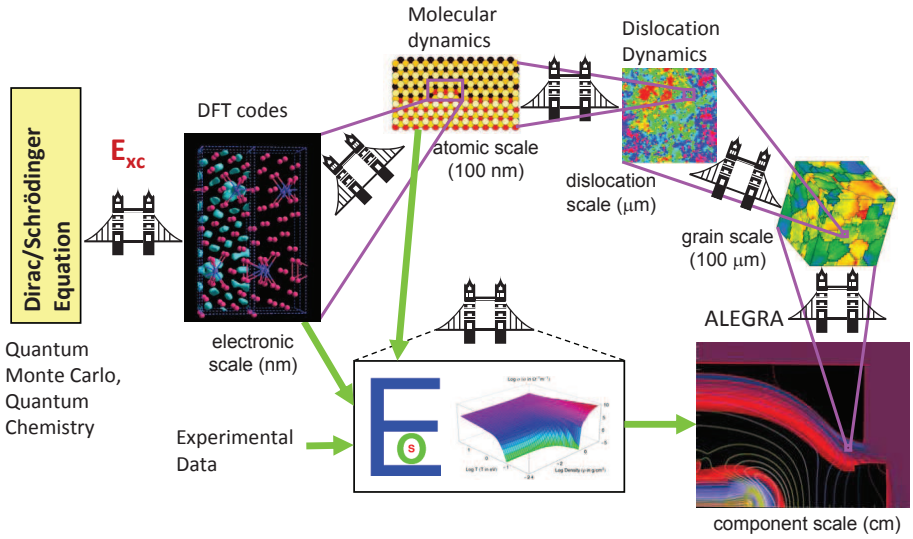

Figure 1.1. The foundation of Science Based Engineering is to build bridges from the fundamental Laws of Nature up to the Engineering codes, bridging several length and time scales. In this figure two different paths are depicted. The upper one is quite complicated and illustrates the general problem of bridging several different scales. The lower path is already in use at Sandia. For Equation of State construction, data provided by Density Functional Theory (DFT) based calculations are used in addition to experimental data. The DFT calculations are used in two ways, either directly or as a provider of forces in a Molecular Dynamics scheme.

bulk matter at equilibrium and at fairly low temperatures. While these pps usually produce very good zero temperature equilibrium lattice constants and bulk moduli, their use in other environments can produce less reliable results. At Sandia we are using the projector augmented-wave (PAW) pseudo-potentials in VASP for shock physics applications. It is well known that both the dense matter and the elevated temperatures in this regime can make these pp results less accurate. The aim of my work on PAW potentials for VASP is to understand and remedy the limitations of standard VASP potentials.

Chapter 2

Density Functional Theory

Density Functional Theory (DFT) is an exact reformulation of the fundamental law of nature governing the behavior of electrons. If electrons are in materials with heavy ions, the fundamental law is the Dirac equation. For materials composed of lighter ions, the non-relativistic limit of the Dirac equation, the Schrödinger equation, might be used.

Density Functional Theory was first developed using the Schrödinger equation. Using the Hohenberg-Kohn theorem,[6] the Schrödinger equation, which decides the electronic properties of a material via many-body electronic wave-functions, can be cast in the form of the Kohn-Sham (KS) equations, which instead decide the behavior of ground state electrons via auxiliary non-interacting single particle Kohn-Sham orbitals forming the true electron density of the material. The key point is that solving for non-interacting single particles is a much less demanding task than solving for many-body wave-functions.

Despite the theory in itself being exact, approximations for the *Exchange-Correlation functional* still need to be done since the form of this object is unknown. The accuracy of the approximation for the Exchange-Correlation functional is the factor that decides the ultimately attainable accuracy of the calculations. No calculations based on DFT can ever give better results than this approximation allows. If the 'divine'[14] functional were known, however, the KS equations would yield the exact same results as the fundamental law of nature, the Schrödinger Equation.

The KS equations are often interpreted as the equations of electrons moving in a field formed by all the other electrons, so called mean-field theory. From a mean-field theory perspective the KS orbitals can be interpreted as approximations for the true many-body electron wave-functions. This alternative interpretation of the KS equations can be very fruitful if handled correctly, but it also has created, and is creating, a lot of confusion in the field. In Figure 2.1 we try to compare the two views. In addition to the 'pure' KS equations, several mean-field theory based schemes are also implemented in VASP.

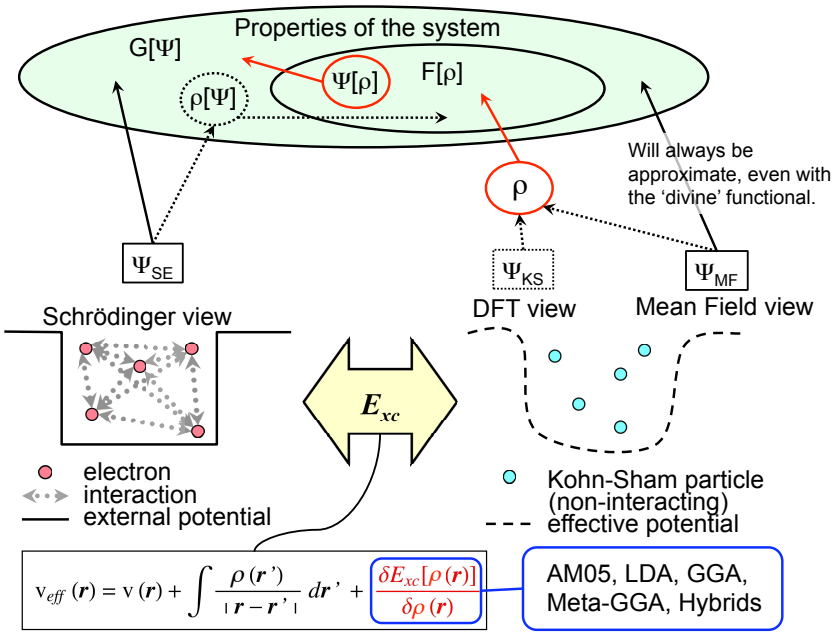

Figure 2.1. The exact functional would give the exact density, ρ, and thus the exact properties via density functionals, $F[\rho]$. The unknown wave function density functional, $\Psi[\rho]$, would in this case give all properties that can be calculated from the Schrödinger equation exactly. However, the mean field view of using the KS orbitals as approximate electron wave functions would be approximate. Only the density and properties calculated via density functionals are guaranteed to be exact. The quality of a functional can thus not be judged by how well it reproduces wave function derived properties. From Reference 13.

Chapter 3

The Projector Augmented Wave method

The computational advantages of the DFT method are further advanced by combining it with a pseudo-potential method. In contrast to the approximate exchange-correlation functionals, a pseudo-potential approximation is a numerical one. The results obtained with a pseudo-potential should give the exact same results as an all-electron calculation, *provided the same exchange-correlation functional is used*.

The projector augmented-wave (PAW) method was developed by Blöchl in 1994.[2] The version of the PAW method implemented in VASP is thoroughly described in Reference 11 and the PAW potentials produced for this method are now the only recommended ones for use in VASP. A library of functional-specific PAW potentials is distributed together with the source code. The distribution deployed in April 2012 contains many 'GW PAWs' which are of special interest to the Sandia shock physics community.

Pseudo-potentials can also be used in many-body schemes based on the mean-field view of the KS equations (see Fig. 2.1). One such method of relevance for this work is the GW method. This method uses the unoccupied states (which have no real meaning in DFT since they do not contribute to the density) and it has been noted that PAWs that give very accurate ground state properties still can produce highly deficient unoccupied states. Since the Fermi-Dirac distribution of electrons at high temperatures distributes electrons also to states that are unoccupied at zero temperature, where pseudo-potentials are constructed, we have noted that using the GW PAWs improves the quality of calculations for high-temperature shock physics applications.

The many components of a PAW potential for VASP are contained in a file named POTCAR. The individual components are well described in section "IV. PAW DATASETS" in Reference 11. A computer program generating POTCAR files have been provided to me by the main VASP developer, Dr. George Kresse, who has also produced all the standard PAW potentials distributed with VASP. The generator program takes a minimum of two input files, V_RHFIN and PSCTR, and there are at least 30 parameters that can be set in those files. This report will not concern all of them. However, for the understanding of the results and insights presented below, a few of these parameters need to be discussed. At the beginning of each POTCAR file is an information section stating the values of relevant parameters. Note that, although the VASP default units are Ångström (Å) and electron

Volt (eV), lengths in this section are in bohr, if not otherwise specified.

The all-electron calculation

A pseudo-potential is constructed from an all-electron calculation on a single, free, atom. The aim is to obtain a pseudo-potential that in a pseudo-potential calculation would reproduce selected all-electron results for this atom.

Atom configuration

Contained in the PAW generator program is thus an all-electron DFT code that produces wave-functions and eigenvalues for a spherically symmetric atom. However, in many cases we need to have higher angular momentum components available in a VASP calculation, even though these states are not occupied in an atom. One example is the higher angular momentum state often used to produce the local potential (see below). Sometimes, we also want to use an excited atom as the bases for the PAW construction; this is the case for most of the Li PAWs discussed in Reference 15. The input to the all-electron calculation in the PAW generation is contained in the V_RHFIN file. In POTCAR files produced with the newer versions of the PAW generator code, such as the version I have used in this work, the atomic configuration is printed in the information section at the beginning of the file.

The exchange-correlation functional

The all-electron calculation performed in the process of generating the pseudo-potential is using a specific exchange-correlation functional. This is also specified in the V_RHFIN file. In general a pseudo-potential is functional specific and should not be used with another functional. However, the PAW implementation used in VASP is very insensitive to the functional used in producing the PAW, and from version 5 of VASP accurate results can be obtained with any implemented functional used on the standard LDA or PBE[20] PAW potentials. In Reference 16 we show that both LDA and PBE[20] PAWs can be used together with AM05[1] in VASP 5, giving nearly identical results. This allows the use of new functionals in VASP 5 without the substantial work of generating functional specific pps. Many of the calculations at Sandia are made using both LDA and AM05, and we have thus been focusing on making LDA PAWs for use in shock physics applications. The functional used in the production of the PAW is written in the information section as the value of the tag LEXCH. Note that the value CA ('Ceperly and Alder parameterized by J.Perdew and Zunger') denotes LDA with the Perdew-Zunger correlation,[19] which is fitted to the Ceperly and Alder Quantum Monte-Carlo results for the uniform electron gas.[4]

The number of valence electrons

A crucial decision to make in the PAW construction is how many of the electrons should be classified as core or valence. The core electrons in a PAW potential are represented as core charge densities based on the atomic calculation. As long as the core electrons in a VASP calculation are still atomic like and inert, that is, they do not participate in the binding, this is a good approximation. However, as matter is compressed, core electrons that at equilibrium are inert, can start to participate in the binding of the material, thus becoming valence electrons. Another problematic case is at very high temperatures, when core electrons might need to be promoted to higher energy states according to the Fermi-Dirac distribution. This is a very strong limitation of a pseudo-potential and no calculation can be trusted in the regime where electrons assumed to be inert in a PAW potential actually are not. The solution to this problem is to design PAW potentials that promote some of the atomic core electrons to valence electrons. The number of core vs valence electrons are also set in the V_RHFIN file. The very first number after the name of the PAW potential in the POTCAR file is the number of valence electrons.

The PAW generation

The first and most important criteria for a good PAW potential is that it reproduces the most important results of the all-electron calculation on the single, free, atom. There is no hope to be able to mimic all-electron results for more complicated systems if the PAW potential cannot at least reproduce the atomic properties. Theoretically, the PAW method is able to exactly reproduce the all-electron wave-functions of the *valence electrons*, but in practice this is never attainable. By evaluating the logarithmic derivatives of the atomic pseudo wave-functions and compare them to the logarithmic derivatives of the exact atomic wave-functions produced in an all-electron calculation, the quality of the scattering properties can be assessed. The PAW generator code is printing out logarithmic derivatives of the atomic wave-functions from the all-electron, the bare pseudo-potential, and the full PAW calculations in a file named DDE. In the previous distribution of PAW potentials, this DDE file was given together with the POTCAR, the V_RHFIN, the PSCTR, and a file with the all-electron atomic potential, named V_TABIN (used to speed up the all-electron atomic calculations by giving a good input potential for the self-consistent loop). The DDE file is the main tool for tuning the parameters in the PSCTR file for obtaining an accurate PAW potential. A good correspondence between the all-electron and the PAW logarithmic derivatives is a necessary but not sufficient criteria for a good PAW potential.

The logarithmic derivatives are calculated at a specified distance from the atom center. This radius is given in the POTCAR information section as RWIGS. In newer versions of the generator code the value of RWIGS can be set to any value without influencing any other setting, thus, the rest of the POTCAR file is independent of this value. However, this value is still a good indicator as to the smallest nearest neighbor distance at which the PAW potential can be trusted. More stringent restrictions of the maximum compression at

which the PAW potential can be trusted are set by the various cutoff radii used in the PAW construction. The RWIGS value is usually set slightly larger than the largest of these radii. Examples of logarithmic derivative plots are shown in Figure 4.1 and they will be discussed further below.

The basic idea with a pseudo-potential is to smoothen out the rapidly varying wave-functions near the atomic center, permitting the use of a smaller basis to resolve the variations of the pseudo-wave functions compared to the all-electron wave functions. The basis size in a plane-wave code is determined by the kinetic energy cutoff (ENMAX in the POTCAR file, but ENCUT in the calculation input file, INCAR). The computational cost of a calculation is highly dependent on this cutoff energy. Standard PAW potentials are constructed with both accuracy and speed in mind, and while accuracy demands smaller radii, speed requires larger, and the final choice of radii will always be a compromise. However, for the applications we are interested in for this work, the primary focus is on accuracy, not the speed of the calculations.

The local potential

The local potential is used for all angular momentum channels that do not have their own projectors or pseudo-potentials. It can be constructed from either 1) a higher angular momentum pseudo-potential or 2) an independent pseudized construction based on the all-electron potential. In both cases the local potential outside of a certain radius is equal to the self-consistent, all-electron potential while it is modified inside this radius. The first case is used if the tag ICORE is set. The value of ICORE is the angular momentum channel that is used as the local potential and its radius can be found in the last line of the "Description" part of the information section in POTCAR (which should, of course, have the same angular momentum, l, as the ICORE value). In the second case the cutoff radius is shown by the RCLOC tag. The harder (having smaller radius) this local potential is the better description of the scattering properties we get. After all, if the radius is 0 we recover the all-electron potential. However, the harder we make the local potential, the easier it is to have unphysical "ghost" states appearing. Signs of ghost states sometimes can be seen already in the DDE plots, but sometimes only further testing, such as the Density of States (DOS) calculations discussed below, reveals them.

Partial wave cutoffs

A PAW potential contains partial waves and projectors. These are constructed from all-electron wave-functions obtained in the all-electron calculation. There are two types of wave-functions used: wave-functions calculated at the atomic eigenenergies, and wave-functions calculated at non-eigenenergies. In both cases pseudo-wave functions are constructed by pseudizing inside a specified radius.

The values of the energies and the cutoff radii for the partial waves are listed in the

"Description" part of the information section in the POTCAR file. The largest of the cutoff radii is also listed in the RCORE tag. This value is a good indicator of the limit at which further compression would cause accuracy concerns.

Number of projectors

The energies and radii of the partial waves and the number of projectors are determined by examining the DDE plots. The simple rule is that you add a projector if the desired accuracy can not be obtained with the current set. However, determining the energy of this added projector is a highly non-linear process, and some amount of trial-and-error is usually needed. Since harder potentials generally are more accurate, fewer projectors are usually needed for those PAW potentials. However, for improving the scattering properties in the higher energy range required for high temperature calculations, more projectors are needed. Having more than 3 projectors with the same angular momentum is very hard to achieve, this problem is similar to the problem of over-complete basis sets in all-electron codes. A general observation is that constructing PAW potential encompasses many of the same problems and questions as constructing accurate basis sets for all-electron codes.

The valence compensation charge

Claims have been made that the introduction of valence compensation charges into the VASP PAW scheme is problematic (see Reference 7 and references therein). It seems this problem, if present, is small in LDA PAWs and in fact I see no sign of any problems that might be attributed to the presence of compensation charges. However, I have also taken great care in using an appropriate setting for the dense augmentation grid. I routinely use an augmentation grid energy cutoff (ENAUG) double that of the plane-wave grid specified by ENCUT. The compensation charge radius, RDEPT, should be comparable to other cutoff radia.

The partial core corrections

It has long been known that substantial errors can be obtained in results using pps stemming from the non-linear dependence on the density in the exchange-correlation energy:

$$(n_{valence} + n_{core})^{\frac{5}{3}} \neq n_{valence}^{\frac{5}{3}} + constant \quad . \tag{3.1}$$

Louie *et. al.*[12] introduced non-linear core corrections in order to mitigate this problem while keeping the computational advantages of the pps themselves. The partial core correction is constructed from the all-electron atomic core charge in the atomic all-electron calculation done while generating the pp. The partial core density is equivalent to this all-electron core charge outside of a radius RPACOR, given in the header of the POTCAR file.

Chapter 4

The standard Mo PAWs

A Mo atom has 42 electrons. Most of these electrons are usually not participating in the bonding of a material and can be treated as core electrons and be represented with a pseudo potential. The minimum number of valence electrons needed for an accurate bonding picture is the outermost 5 atomic $4d$-electrons and the single atomic $5s$-electron, that is, 6 electrons. For high temperature and density also the remaining forth shell electrons, 2 $4s$ and 6 $4p$, might be needed in the valence.

The library of standard PAW potential deployed in April 2012 (version 52) contains 4 Mo LDA PAWs. One, Mo, has 6 electrons in the valence, one, Mo_pv, is a 12-electron potential, and the last two, Mo_sv and Mo_sv_GW, are 14-electron potentials, thus having all fourth shell electrons in the valence. While the Mo_sv potential is based on the ground-state electron configuration, the Mo_sv_GW potential is based on an atom with the single $5s$ electron promoted to a $4d$ state. Contrary to the Li PAWs studied before,[15] all these PAWs have a substantial number of electrons in the core, introducing the necessity of, for example, partial core corrections.

The library of standard PAW potential for VASP5 available before April 2012 also contained 4 Mo LDA PAWs. None of them was labeled with GW. Mo, Mo_pv_new, and Mo_sv, correspond to Mo, Mo_pv, and Mo_sv, respectively, in the newer distribution. However, they do differ by a rotation between the projectors and I have thus performed selected calculations with both versions. In this distribution, the TITEL field in Mo indicates a PBE potential, but in reality it is generated with LEXCH = CA, thus it is an LDA potential. To distinguish between the Mo_pv potentials in the old and new distributions they are labelled with a year suffix, see Table 4.1.

The even older distribution contained 3 Mo PAW potentials: Mo, Mo_pv, and Mo_sv. The Mo and Mo_pv potentials are exactly the same as the Mo and Mo_pv in the newer, before-April-2012, distribution, while the Mo_sv potentials differ significantly. In all the only potential still in use from this distribution is the Mo one.

Four standard PAW potentials

I have chosen to examine more closely the 4 PAW potentials in the April 2012 distribution and the Mo_pv from the before April 2012 distribution (thus omitting only the oldest distribution Mo_sv). The essential details of the standard potentials are given in Table 4.1.

Table 4.1. All lengths in bohr and all energies in eV. The RDEPT values given in parenthesis are determined from the last number in the line after 'PAW radial sets' in the POTCAR file (see Reference 15). The RDEPT in the line after 'PAW radial sets' is part of the radial grid and set to the first value belonging to the grid that is >= (RDEPT in the header).

Name in this report	Mo	Mo_pv_02	Mo_pv_05	Mo_sv	Mo_sv_GW
v52 April 2012 directory name	Mo	—	Mo_pv	Mo_sv	Mo_sv_GW
Pre April 2012 directory name	Mo	Mo_pv	Mo_pv_new	Mo_sv	—
Even older directory name	Mo	Mo_pv	—	—	—
TITEL	PAW Mo 08Apr2002	PAW Mo_pv 08Jan2002	PAW Mo_pv 04Feb2005	PAW Mo_sv 29Jan2005	PAW Mo_sv_GW 23Mar2010
Valence electrons	6 ($4d^5 5s$)	12 ($4p^6 4d^5 5s$)	12 ($4p^6 4d^5 5s$)	14 ($4s^2 4p^6 4d^5 5s$)	14 ($4s^2 4p^6 4d^6$)
RWIGS	2.750	2.750	2.750	2.750	2.600
ENMAX	224.535	224.535	224.535	236.514	311.692
EAUG	345.278	392.427	392.427	446.014	848.831
RCLOC or ICORE/RCUT	2.111	1.902	3/2.600	3/2.500	1.608
RCORE	2.750	2.600	2.700	2.500	2.300
RDEPT	2.193	2.124	(2.179) 2.166	(2.044) 2.031	1.787
RPACOR	2.200	2.200	2.200	2.200	2.000
s projectors	2.600	2.600	2.700	2.100	1.500
RCUT	2.600	2.600	2.700	2.400	1.500
	—	—	—	—	1.700
p projectors	2.750	2.500	2.500	2.100	1.800
RCUT	2.750	2.500	2.500	2.100	1.800
d projectors	2.500	2.500	2.500	2.500	2.150
RCUT	2.500	2.500	2.500	2.500	2.150
f projector	—	—	—	—	2.300
RCUT					

The interaction of two atoms positioned within each others cutoff radii can be completely corrupt. This severely limits the accuracy of calculations of compressed matter. It is well known that since the matching of the pseudo-wavefunctions and the all-electron wavefunctions at the RCUT radius is both for the value and the derivative, the pseudo and all-electron wavefunctions usually agree to some smaller radius than RCUT (see Reference 15). I have verified that this radius is at least RCUT/1.2 for all the Li partial waves studied in Reference 15. Based on the RCORE values in Table 4.1 and using the criteria developed from this fact in Reference 15, the potentials should absolutely not be used beyond the bcc densities or nearest neighbor distances given in Table 4.2. It is noted that the RDEPT value for each potential is less than half its nearest neighbor distance given in Table 4.2.

Table 4.2. Maximum bcc density and smallest nearest neighbor distances beyond which the accuracy of the Mo PAWs cannot be guaranteed, determined from the criteria developed in Reference 15. The accuracy of the potentials inside of these limits needs to be determined by more stringent tests. Criteria associated with the frozen core electrons might also need to be considered.

	Mo	Mo_pv_02	Mo_pv_05	Mo_sv	Mo_sv_GW
Bcc Mo density (g/cm^3)	14.50	17.16	15.32	19.30	24.79
Mo-Mo nearest neightbor distance (Å)	2.42	2.29	2.38	2.20	2.03
Mo-Mo nearest neightbor distance (bohr)	4.58	4.33	4.50	4.16	3.83

However, compared with the assessment of the Li PAWs in Reference 15, the Mo PAWs here studied all have core electrons, and radii connected to the core, such as the partial core correction radius, RPACOR, needs to be taken into account as well. If the RPACOR value of 2.2 bohr (the same for all potentials studied here, except the GW one) is used as a half nearest neighbor distance, none of these potentials should be used beyond a Mo-Mo nearest neighbor distance of 4.4 bohr or 2.33 Ångström, or a bcc Mo density of 16.39 g/cm^3. For the GW potential this gives a nearest neighbor distance of 4.0 bohr or 2.12 Ångström, or a bcc Mo density of 21.82 g/cm^3 There is also an assumption in deriving the expression for the Hartree Energy[11] that the pseudized core charge densities (embedded in the local potential) do not overlap. However, this approximation is in line with other approximations made in the PAW method and is usually not a concern. We can assume that this approximation is more severe as core charges overlap more, such as in compression, and a sensible criteria might be to consider the local potential RCUT or RCLOC as an indication of the magnitude of this error. This will be further investigated in the future.

From Table 4.1 it is clear that of the standard potentials Mo_sv_GW should give best scattering properties at smaller radii. In Figure 4.1 I compare the DDE plots for these potentials at the RWIGS radii, which are the same for all potentials except the GW one.

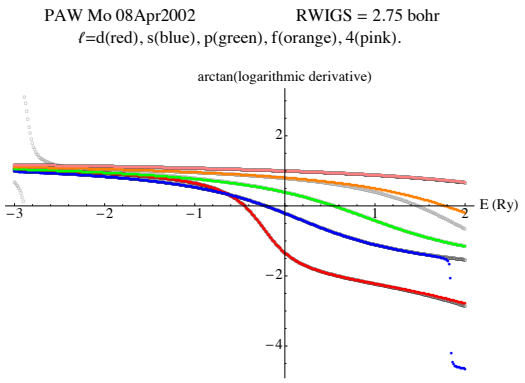

(a) Mo logarithmic derivatives at radius 2.750 bohr.

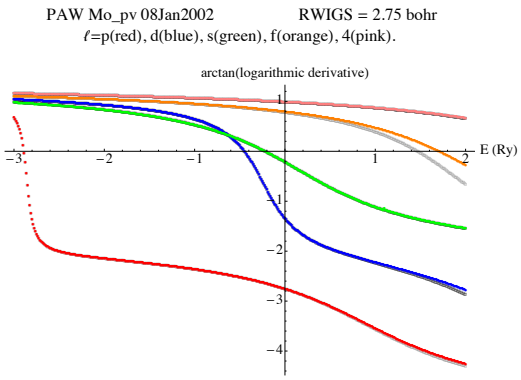

(b) Mo_pv_02 logarithmic derivatives at radius 2.750 bohr.

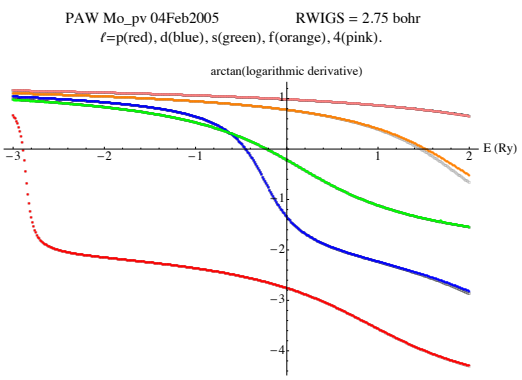

(c) Mo_pv_05 logarithmic derivatives at radius 2.750 bohr.

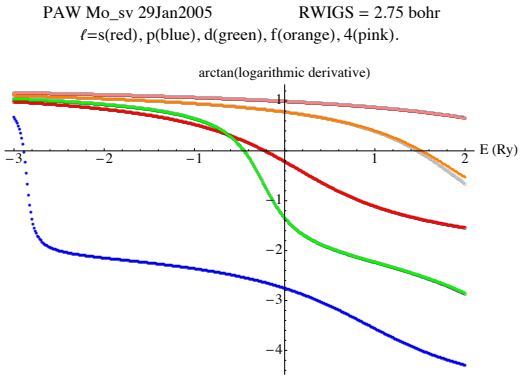

(d) Mo_sv logarithmic derivatives at radius 2.750 bohr.

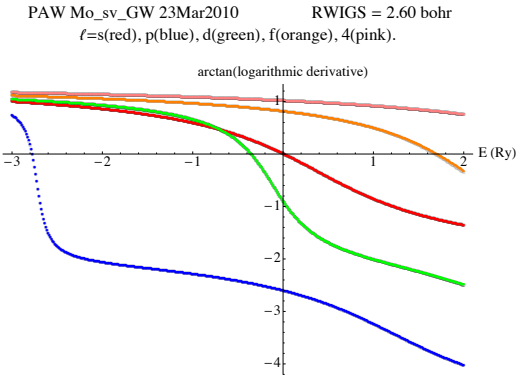

(e) Mo_sv_GW logarithmic derivatives at radius 2.600 bohr.

Figure 4.1. The arctan of the logarithmic derivatives of pseudo wave-functions (colored) compared to those of all-electron wave-functions (black and grey, not seen if the colored points are exactly on top). The RWIGS value of 2.750 (2.600) bohr corresponds to a half nearest neighbor distance in bcc Mo at a density of 8.4 (9.9) g/cm^3.

Since the main differences between the Mo, Mo_pv_02, and Mo_pv_05 potentials are seen already at this RWIGS, I did not check these at any smaller radii. A so called ghost state is clearly seen in the s-channel at around 1.8 Ry in the DDE plot for the Mo potential. There are also indications that there are ghost states in the s-channels of the Mo_pv_02 and Mo_pv_05 potentials, at 1.1 and 1.65 Ry, respectively. (If you read a high resolution pdf version of this report, you might be able to zoom in on the respective sub-figures in Figure 4.1 to see the small blips indicating ghost states).

While the main differences between the potentials are seen in the standard energy interval in Figures 4.1, to emphasize the differences between the Mo_sv and Mo_sv_GW potentials, the logarithmic derivatives at a smaller RWIGS, for energies on a larger energy interval, are shown in Figure 4.2.

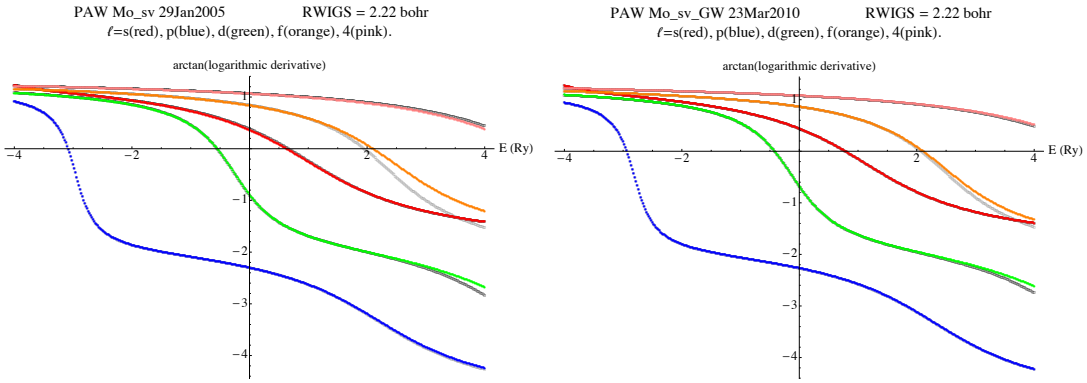

(a) Mo_sv logarithmic derivatives at radius 2.220 bohr.

(b) Mo_sv_GW logarithmic derivatives at radius 2.220 bohr.

Figure 4.2. The arctan of the logarithmic derivatives of pseudo wave-functions (colored) compared to those of all-electron wave-functions (black and grey, not seen if the colored points are exactly on top). The RWIGS value of 2.220 bohr corresponds to a half nearest neighbor distance in bcc Mo at a density of 16 g/cm^3.

In Figure 4.3 the Fermi-Dirac (FD) distribution function for a temperature of 50000 Kelvin is shown. The FD distribution function should be centered at the chemical potential/Fermi level. In the T=0 calculations described in the next Section, the Fermi level was in the range of $0.5 - 1$ Rydberg. Due to the substantial population of states with energies within 1 Ry above the chemical potential at this temperature, the ghost states present in all potentials but the Mo_sv and Mo_sv_GW potentials would disqualify them from use at this elevated temperature (see Figures 4.1).

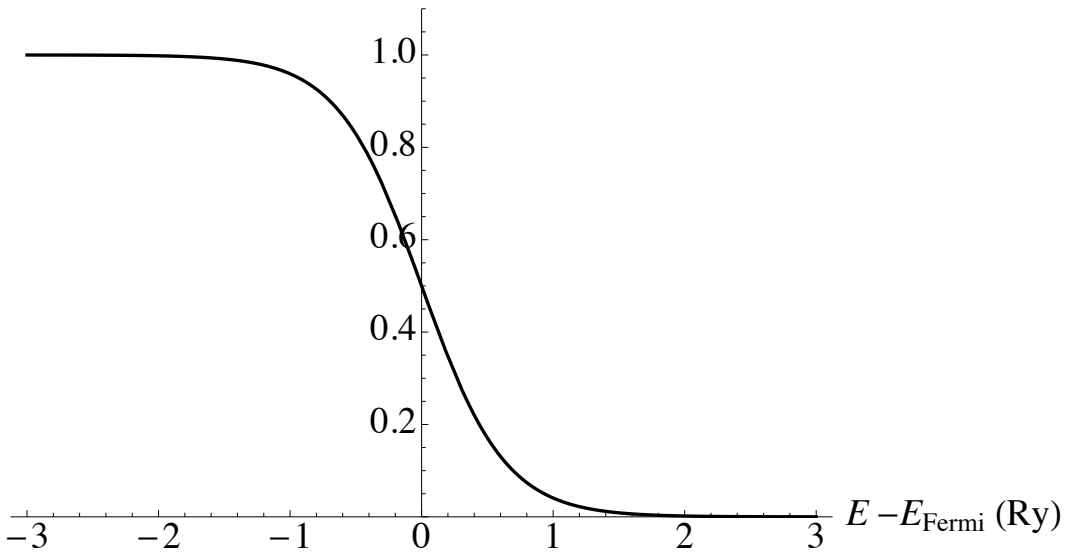

Figure 4.3. The Fermi-Dirac distribution function for a temperature of 50000 Kelvin.

Calculations using the Mo PAW potentials

In order to gain some insight into the limitations of the standard PAW potentials I have performed several sets of calculations. The calculations have been performed using the ab-initio total-energy and molecular-dynamics program VASP (Vienna ab-initio simulation program) developed at the Institut für Materialphysik of the Universität Wien.[10,11]

All calculations are performed with a plane-wave kinetic energy cutoff (ENCUT) of 4080 eV, while the augmentation grid cutoff (EAUG) is 8160 eV. As seen in Table 4.1 this is far above the recommended ENMAX and EAUG. A single test with ENCUT = 500 and EAUG = 1000 gave identical results. All calculations are done with a Γ centered $32 \times 32 \times 32$ Monkhorst-Pack[17] $\boldsymbol{k}$-point mesh which resulted in 969 irreducible $\boldsymbol{k}$-points. All calculations are made with the tetrahedron scheme with Blöchl corrections[3] (ISMEAR = -5)

Equilibrium density

According to the all-electron LAPW results of Haas *et. al.*,[5] that are considered the most accurate calculations of lattice constants to date, the LDA, zero temperature equilibrium bcc lattice constant is 3.116 Ångström. As seen in Figure 4.4, different potentials give slightly

different energy vs lattice constant curves. A fit to the Murnaghan Equation of State[18] gives

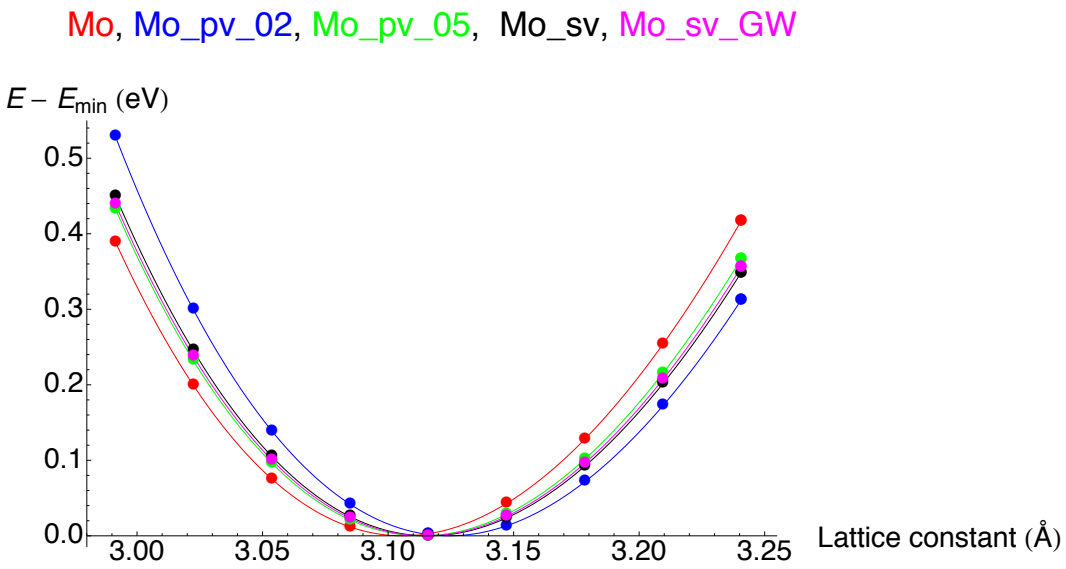

Figure 4.4. Energy versus volume near equilibrium calculated using different PAW potentials.

equilibrium lattice constants and bulk modulii given in Table 4.3, where also results from the all-electron RSPt[22] code are given as benchmarks. The limited accuracy of the Mo PAW

Table 4.3. Equilibrium lattice constants and bulk moduli determined from calculations with the 5 different potentials. Given are also the values obtained with two all-electron methods.

	Mo	Mo_pv_02	Mo_pv_05	Mo_sv	Mo_sv_GW	Wien2k[5,23]	RSPt[22,25]
Lattice constant (Å)	3.106	3.124	3.113	3.116	3.116	3.116	3.119
Bulk modulus (GPa)	300	294	292	289	289	294	288

is evident. The Mo_pv_02 results are just barely within numerical error bars.

Pressure

We can expect the differences between potentials to be more apparent at higher pressures, where the differences in cutoff radii start to influence the results.

On the top of Figure 4.5, I have added a scale expressing the density in half the nearest neighbor (nn2) distance. If the density is such that this distance is smaller than the cutoff radii in the PAW potential we can suspect that the PAW potential might not be accurately describing the system. It should be noted that three of the five standard PAWs investigated in this report are used inside their RCORE distance already at equilibrium (see Table 4.1). Only Mo_sv and Mo_sv_GW have RCORE values smaller than half the nearest neighbor distance at equilibrium, thus safely describing bonding in the bulk system without influence from the core regions. Assuming that the best result is obtained with the Mo_sv_GW PAW, it is clear that the improvement in local potential between the Mo_pv_02 and Mo_pv_05 potentials, seen in Figure 4.1, is crucial for the properties at high compression, overriding the possible decrease in accuracy stemming from the increased cutoff radii in the s projectors.

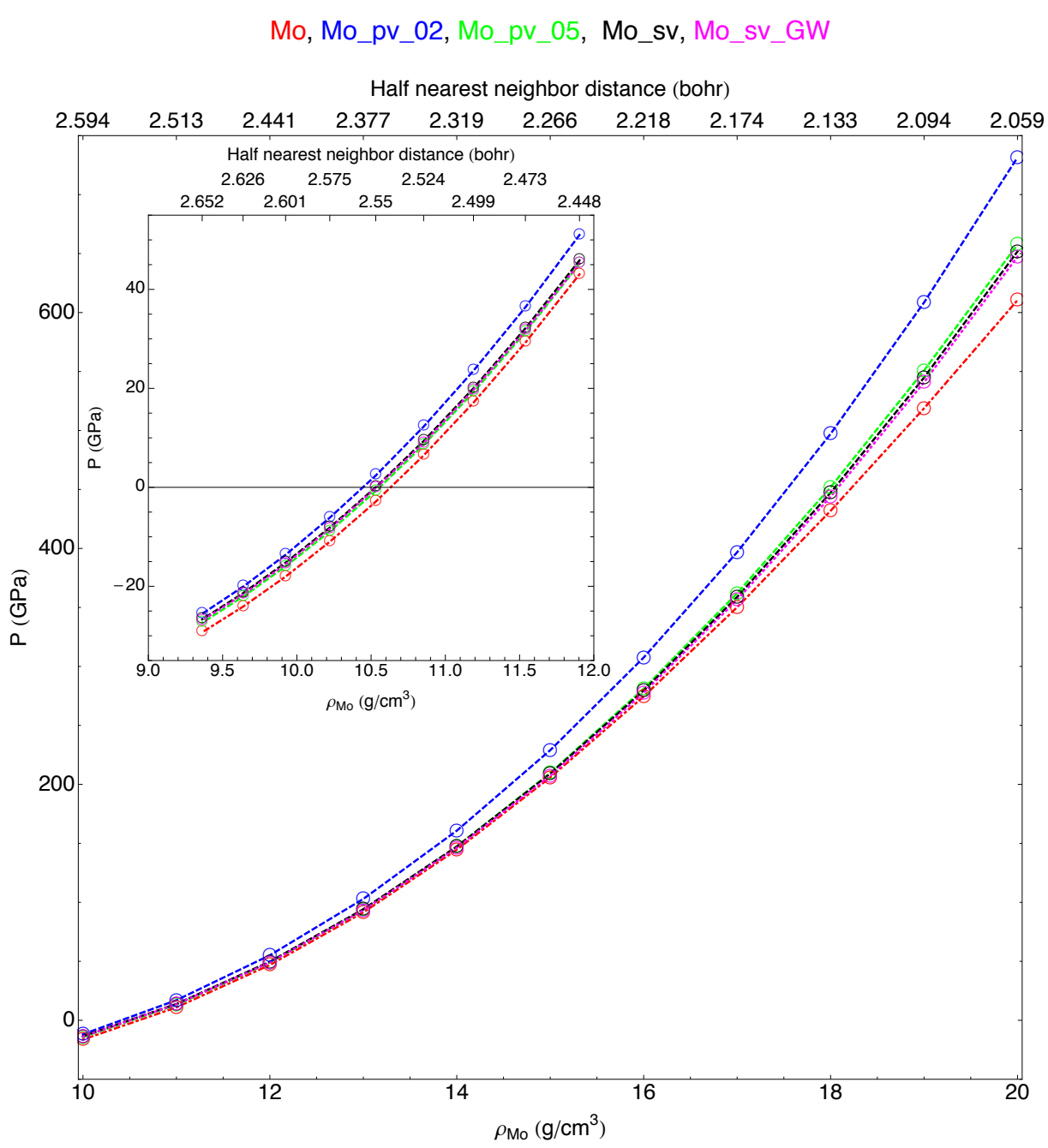

Figure 4.5. The pressure of bcc Mo as a function of density. Note the top scale that gives half the nearest neighbor distance. It is clear that *all* potentials are operating inside their largest core radii in compression, cf. Table 4.1.

Density of States

To address the issue of ghost states I have calculated the density of states (DOS) at different compressions. Ghost states give a DOS that has peaks, and an integrated DOS that has steps, that should not be there, and in order to address this we thus need to know the true DOS for bcc Mo. Dr. John Wills, Los Alamos National Laboratory, used his RSPt[22,24] all-electron, full potential, LMTO code to provide me with reference DOS at two different compressions. The RSPt code has been shown to give the same results as VASP PAWs for equilibrium lattice constants and bulk moduli.[16]

In Figures 4.6, 4.7, 4.8, and 4.9 we compare the DOS of all 5 potentials considered in this work and the DOS given in equivalent RSPt calculations. As seen all PAW potentials give the same DOS for occupied states at equilibrium density (Figures 4.6 and 4.7). While the RSPt DOS is not exactly the same, the peak location and general structure is clearly the same. We probably cannot expect DOS calculated by two so very different methods as the LMTO and PAW methods to correspond to each other better than this. This will, however, be further examined in the future. At energies where the quality of the local potentials starts to affect the results, at around 10 eV or 0.75 Ry, it is clearly seen that the older Mo and Mo_pv_02 results starts to deviate from the RSPt result. The ghost states present in the Mo, Mo_pv_02, and Mo_pv_05, potentials are clearly seen.

At higher densities, Figures 4.8 and 4.9, the older Mo and Mo_pv_02 PAWs gives DOSs that starts to differ from the DOS of the newer Mo_pv_05, Mo_sv, and Mo_sv_GW, and RSPt results already for occupied states. It is however evident from Figure 4.8 that quite similar DOSs still can give rise to substantial differences in pressure, see Figure 4.5. Again, we point out the presence of ghost states in the results with the Mo, Mo_pv_02, and Mo_pv_05, potentials.

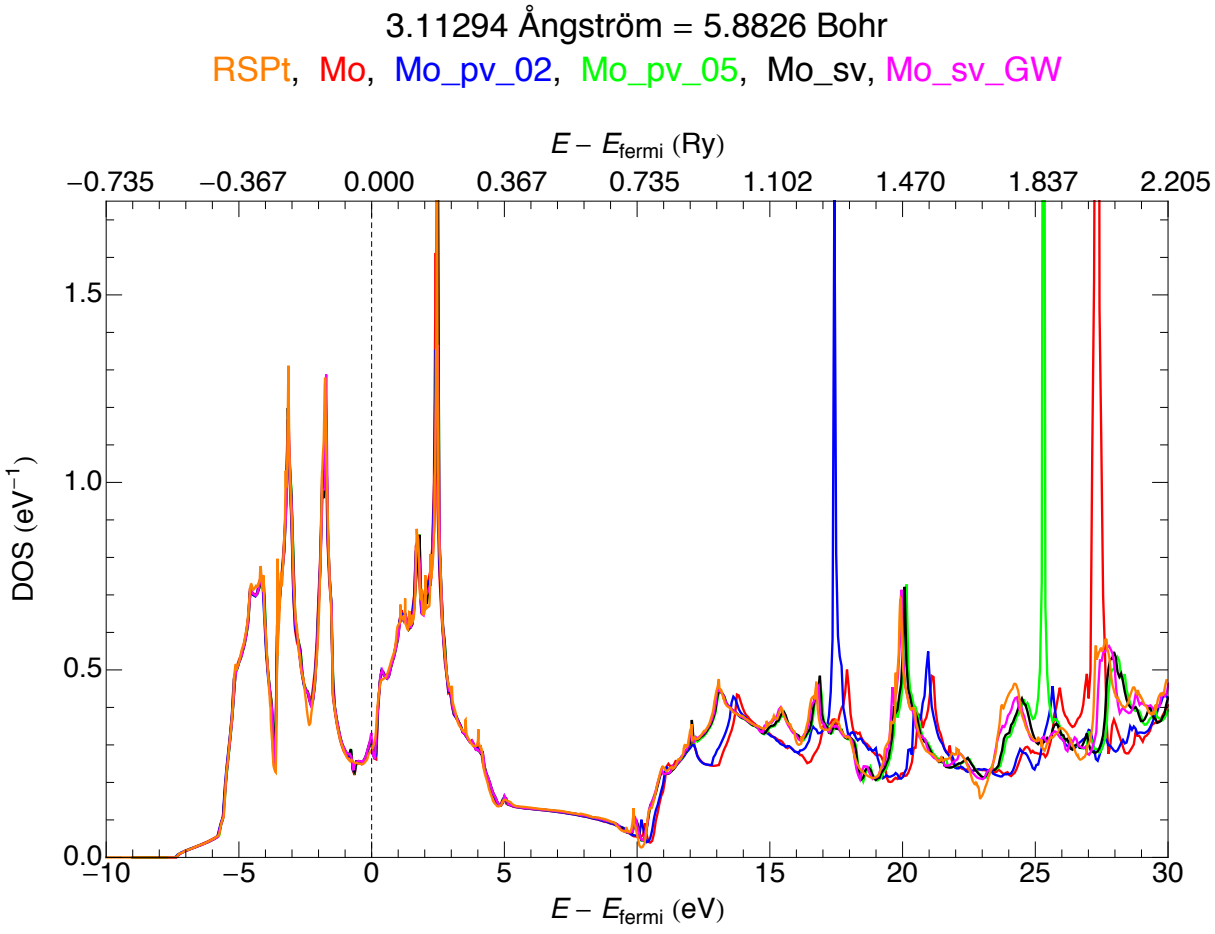

Figure 4.6. DOS at the LDA equlibrium lattice constant calculated using different PAW potentials in VASP and compared to the all-electron RSPt results. Note the ghost states present in the Mo, Mo_pv_02, and Mo_pv_05, PAW potential results.

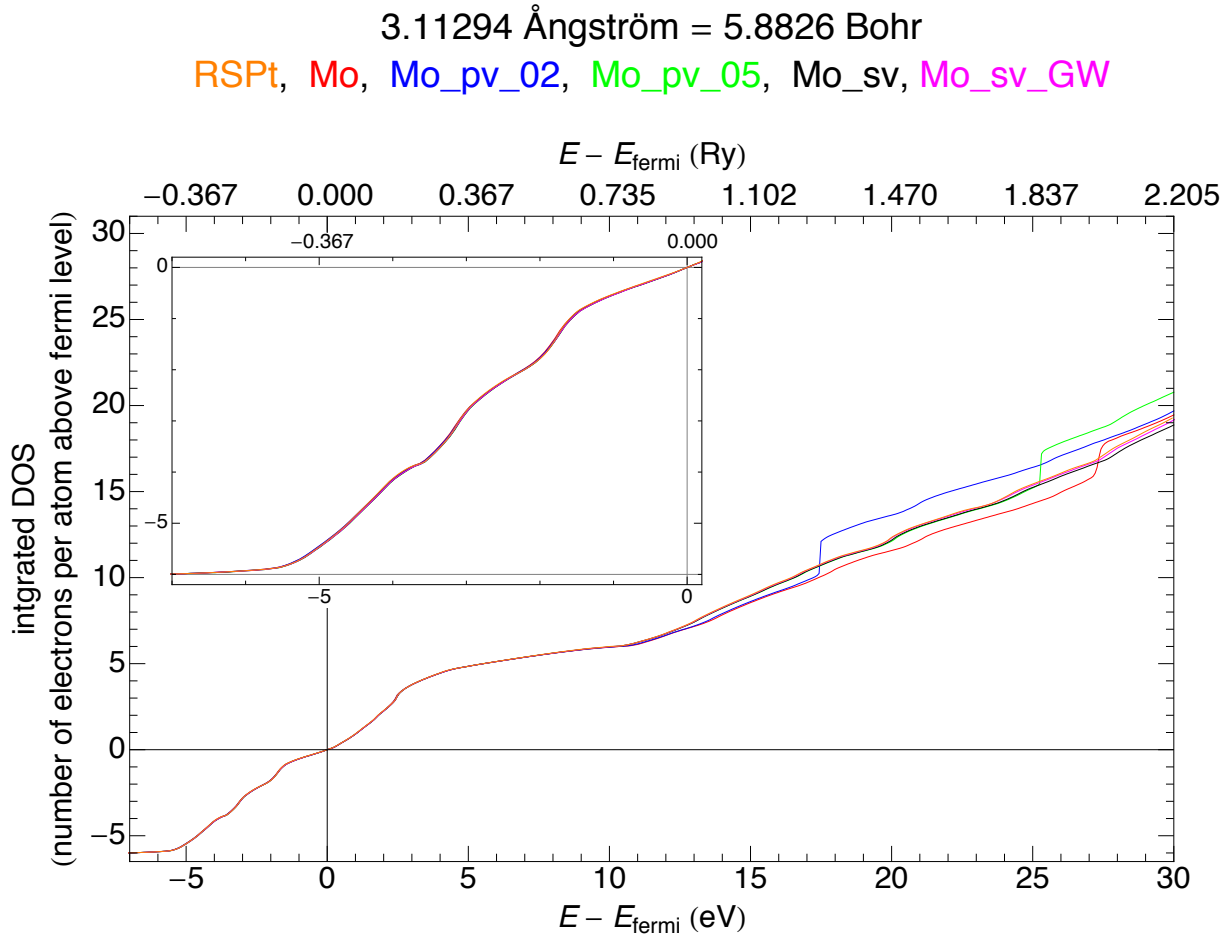

Figure 4.7. Integrated DOS at the LDA equlibrium lattice constant calculated using different PAW potentials in VASP and compared to the all-electron RSPt results. Note the ghost states present in the Mo, Mo_pv_02, and Mo_pv_05, PAW potential results.

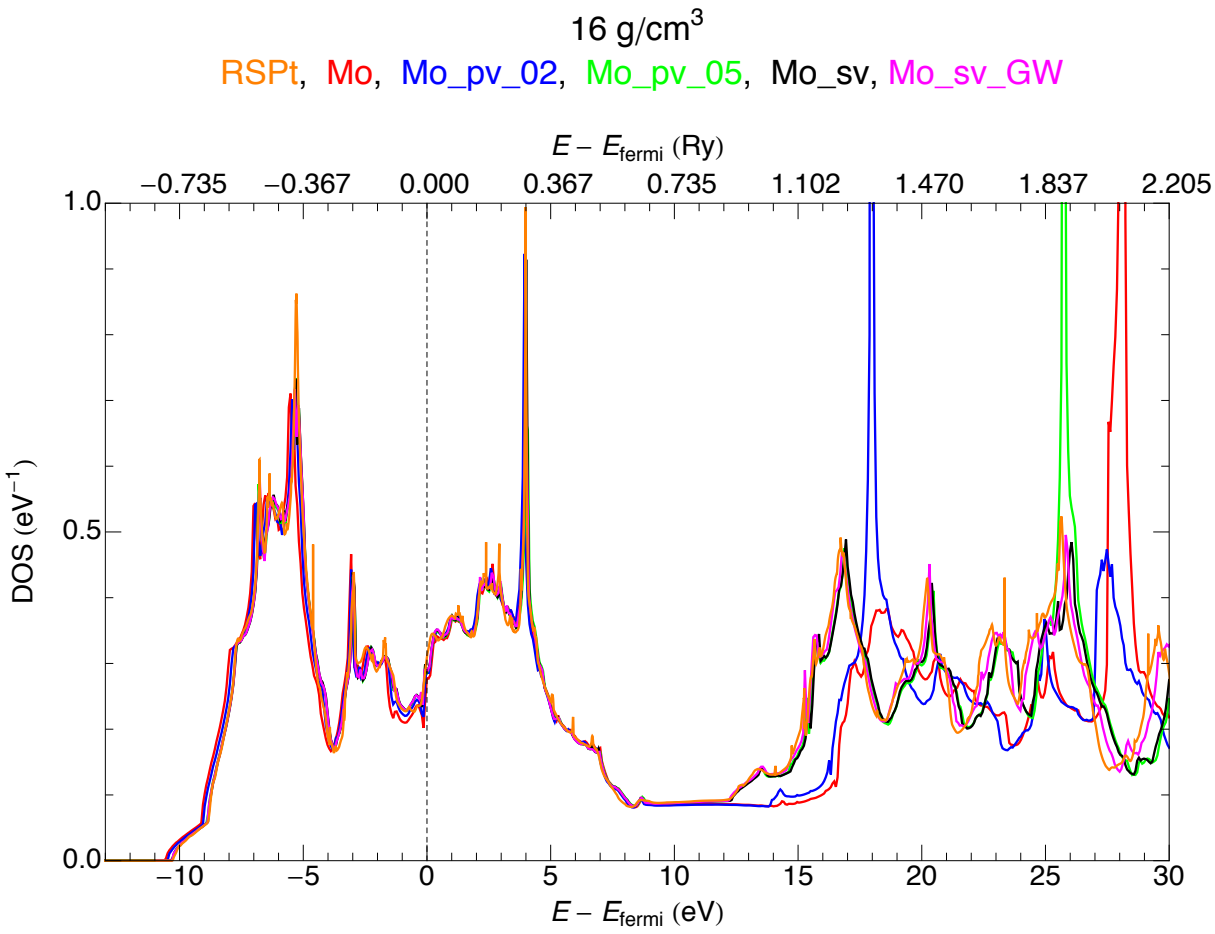

Figure 4.8. DOS at 16 g/cm^3 calculated using different PAW potentials in VASP and compared to the all-electron RSPt results. Note the ghost states present in the Mo, Mo_pv_02, and Mo_pv_05, PAW potential results.

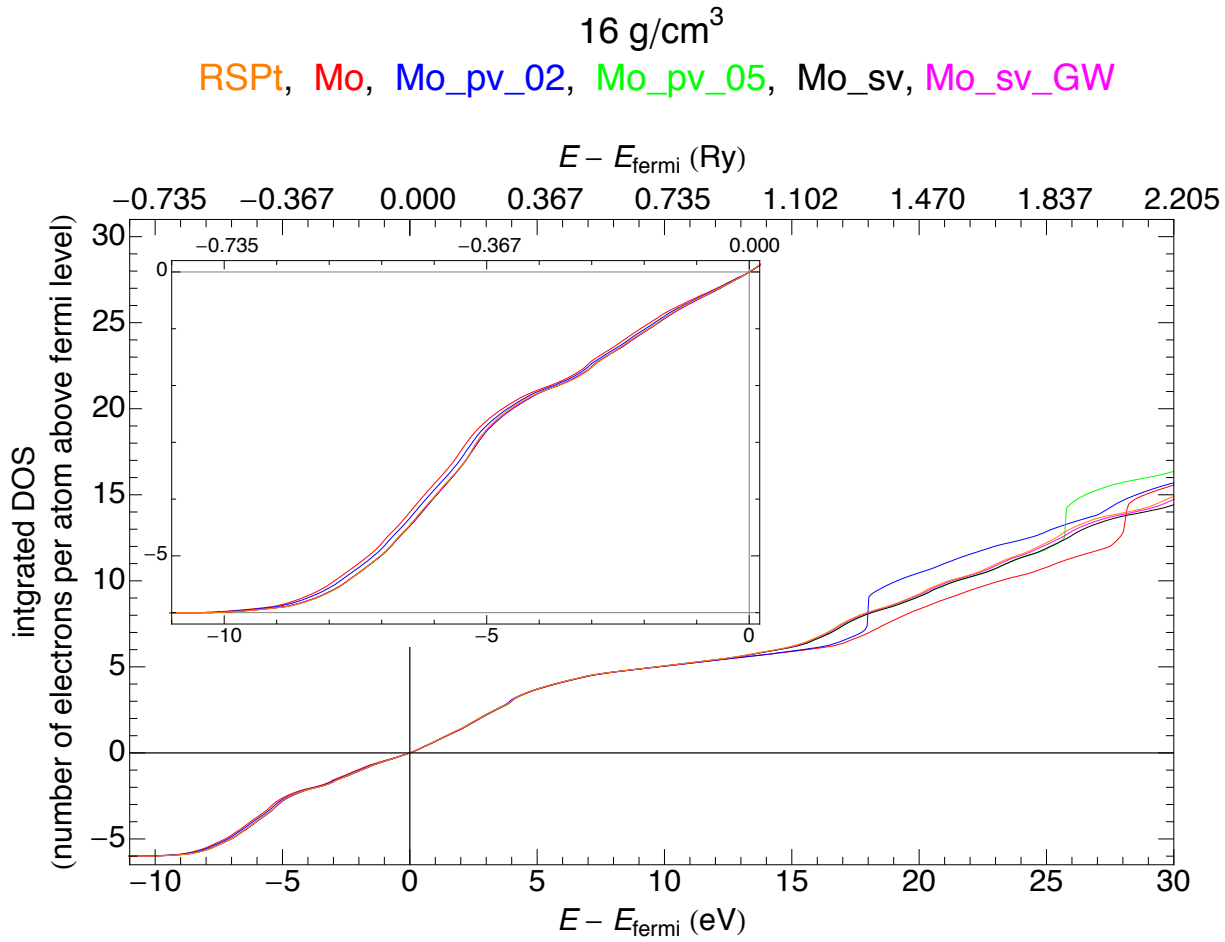

Figure 4.9. Integrated DOS at 16 g/cm^3 calculated using different PAW potentials in VASP and compared to the all-electron RSPt results. Note the ghost states present in the Mo, Mo_pv_02, and Mo_pv_05, PAW potential results.

Chapter 5

Summary and Conclusion

As the codes available for use in Engineering Sciences become more and more sophisticated, materials models used in these codes need to be increasingly accurate. Sandia scientists are at the forefront of DFT-based EOS construction, where experimental information is augmented with information obtained in computational investigations, in order to achieve improved accuracy. The success of the Sandia effort is based on insights and development obtained via studies such as this.

In a pseudo-potential code, such as the Vienna *ab-initio* simulation package (VASP), every atom needs to be described by a pseudo-potential. While other calculational settings, such as $\boldsymbol{k}$-point sampling and plane wave basis size, can be tuned at will, these pseudo-potentials are constructed outside of the computational code and need to be provided as input to the calculation. If the accuracy of a provided pseudo-potential is not enough for the application at hand, another one needs to be constructed.

In this study five molybdenum projector augmented wave (PAW) potentials distributed together with VASP have been investigated and their range of applicability determined. Three of the potentials have ghost states and thus should not be used, at least not for high temperatures. Some of the potentials are available in several distributions, differing by their real space optimization. The older distributions are usually using automatic real space optimization based on the default cutoff, while the newer use no real space optimization. I have found no difference in results using one or the other.

I recommend the use of the Mo_sv_GW potential for densities of bcc Mo up to around 22 g/cm^3, or Mo-Mo nearest neighbor distances of 4.0 bohr or 2.1 Ångström. The Mo_sv_GW potential can probably be used at high temperatures: It is not clear at this point if the discrepancies between the Density of States of this potential and the RSPt ones seen in Figures 4.6 - 4.9, are the due to deficiencies in one or the other method, or in both. *Cautious* use of the Mo_sv potential could also be motivated, for densities of bcc Mo up to around 16.5 g/cm^3, or Mo-Mo nearest neighbor distances of 4.4 bohr or 2.3 Ångström. I would be very careful about very high temperature results, however, based on the discrepancy of its Mo bcc DOS with the RSPt results, seen in Figures 4.6 - 4.9 at around 16 eV or 1.2 Ry. It is easy to plot the Fermi-Dirac distribution given the temperature and the chemical potential from an actual VASP calculation, and I suggest doing this and making sure that not too many states are substantially occupied above 16 eV or 1.2 Ry.

References

[1] R. Armiento and A. E. Mattsson. Functional designed to include surface effects in self-consistent density functional theory. *Phys. Rev. B*, 72:085108, Aug 2005.

[2] P. E. Blöchl. Projector augmented-wave method. *Phys. Rev. B*, 50:17953–17979, Dec 1994.

[3] Peter E. Blöchl, O. Jepsen, and O. K. Andersen. Improved tetrahedron method for brillouin-zone integrations. *Phys. Rev. B*, 49:16223–16233, Jun 1994.

[4] D. M. Ceperley and B. J. Alder. Ground state of the electron gas by a stochastic method. *Phys. Rev. Lett.*, 45:566–569, Aug 1980.

[5] Philipp Haas, Fabien Tran, and Peter Blaha. Calculation of the lattice constant of solids with semilocal functionals. *Phys. Rev. B*, 79:085104, Feb 2009.

[6] P. Hohenberg and W. Kohn. Inhomogeneous electron gas. *Phys. Rev.*, 136:B864–B871, Nov 1964.

[7] Valentin V. Karasiev, Travis Sjostrom, and S. B. Trickey. Comparison of density functional approximations and the finite-temperature hartree-fock approximation in warm dense lithium. *Phys. Rev. E*, 86:056704, Nov 2012.

[8] M. D. Knudson and M. P. Desjarlais. Shock compression of quartz to 1.6 TPa: Redefining a pressure standard. *Phys. Rev. Lett.*, 103:225501, Nov 2009.

[9] W. Kohn and L. J. Sham. Self-consistent equations including exchange and correlation effects. *Phys. Rev.*, 140:A1133–A1138, Nov 1965.

[10] G. Kresse and J. Furthmüller. Efficient iterative schemes for *ab initio* total-energy calculations using a plane-wave basis set. *Phys. Rev. B*, 54:11169–11186, Oct 1996.

[11] G. Kresse and D. Joubert. From ultrasoft pseudopotentials to the projector augmented-wave method. *Phys. Rev. B*, 59:1758–1775, Jan 1999.

[12] Steven G. Louie, Sverre Froyen, and Marvin L. Cohen. Nonlinear ionic pseudopotentials in spin-density-functional calculations. *Phys. Rev. B*, 26:1738–1742, Aug 1982.

[13] Rudolph J. Magyar, Ann E. Mattsson, and Peter A. Schultz. Some practical considerations for density functional theory studies of chemistry at metal surfaces. In Thomas C. Allison, Orkid Coskuner, and Carlos A. González, editors, *Metallic Systems: A Quantum Chemist's Perspective*. CRC Press, Boca Raton, London, New York, 2011.

[14] Ann E. Mattsson. In pursuit of the "divine" functional. *Science*, 298(5594):759–760, 2002.

[15] Ann E. Mattsson. A lithium projector augmented wave potential suitable for use in VASP at high compression and temperature. Technical report SAND2012-7389, Sandia National Laboratories, Albuquerque, New Mexico 87185 and Livermore, California 94550, September 2012.

[16] Ann E. Mattsson, Rickard Armiento, Joachim Paier, Georg Kresse, John M. Wills, and Thomas R. Mattsson. The AM05 density functional applied to solids. *Journal of Chemical Physics*, 128(8):084714, 2008.

[17] Hendrik J. Monkhorst and James D. Pack. Special points for brillouin-zone integrations. *Phys. Rev. B*, 13:5188–5192, Jun 1976.

[18] F. D. Murnaghan. The compressibility of media under extreme pressures. *Proc. Natl. Acad. Sci.*, 30:244, 1944.

[19] J. P. Perdew and Alex Zunger. Self-interaction correction to density-functional approximations for many-electron systems. *Phys. Rev. B*, 23:5048–5079, May 1981.

[20] John P. Perdew, Kieron Burke, and Matthias Ernzerhof. Generalized gradient approximation made simple. *Phys. Rev. Lett.*, 77:3865–3868, Oct 1996.

[21] Seth Root, Rudolph J. Magyar, John H. Carpenter, David L. Hanson, and Thomas R. Mattsson. Shock compression of a fifth period element: Liquid xenon to 840 GPa. *Phys. Rev. Lett.*, 105:085501, Aug 2010.

[22] The RSPt code. See http://fplmto-rspt.org/.

[23] Fabien Tran, Robert Laskowski, Peter Blaha, and Karlheinz Schwarz. Performance on molecules, surfaces, and solids of the Wu-Cohen GGA exchange-correlation energy functional. *Phys. Rev. B*, 75:115131, Mar 2007.

[24] J. M. Wills, O. Eriksson, M. Alouani, and D. L. Price. Full potential LMTO: Total energy and force calculations. In H. Dreysse, editor, *Electronic Structure and Physical Properties of Solids: The Uses of the LMTO Method*, volume 535 of *Lecture Notes in Physics*. Springer-Verlag, Berlin, 2000.

[25] John M. Wills. Private communication.

DISTRIBUTION:

1 Univ.-Prof. Dipl.Ing. Dr. KRESSE Georg
Computational Materials Physics
Faculty of Physics
University of Vienna
Sensengasse 8/12
A-1090 Wien
AUSTRIA
(electronic copy)

1 MS 0747 Veena Tikare, 01444 (electronic copy)

1 MS 1189 Michael P. Desjarlais, 01600 (electronic copy)
1 MS 1189 Thomas R. Mattsson, 01641 (electronic copy)

1 MS 1320 Samuel Scott Collis, 01440 (electronic copy)

1 MS 1322 Ann E. Mattsson, 01444 (electronic copy)

1 MS 0899 Technical Library, 9536 (electronic copy)

Sandia National Laboratories